

# Micro Electrochemical Gas Sensor for selective detection of Volatile Organic Pollutant

Pierre-Alexandre Gross<sup>\*1,3</sup>, Tom Larsen<sup>1</sup>, Frédéric Loizeau<sup>1</sup>, Thomas Jaramillo<sup>2</sup>, Denis Spitzer<sup>3</sup> and Beth L. Pruitt<sup>1</sup>

<sup>1</sup> Microsystems Lab, Stanford Department of Mechanical Engineering, USA

<sup>2</sup> Jaramillo Group, Stanford Department of Chemical Engineering, USA

<sup>3</sup> NS3E, UMR 3208 ISL/CNRS/UNISTRA, France.

\*E-mail: pialgr@stanford.edu

This paper presents the fabrication and working principle of an electrochemical gas sensor for the selective detection of organic molecules dissolved in the gas phase. The sensor is composed of two Pt electrodes where redox reactions occur, and a proton exchange membrane to conduct  $H^+$  from one electrode to the other. The proton exchange membrane in this work is a spin coated *Nafion*® layer. An underlying SU-8 layer assures a double role of adhesion of the *Nafion* to the substrate and water reservoir to limit dehydration of the *Nafion*. The sensor is characterized for its electrochemical properties and tested for the detection of CO as model pollutant. The detection tests are performed in the form of cyclic voltammetry, and show that the sensor can potentially discriminate organic species by their redox potential by showing the presence of the oxidation peak of CO into  $CO_2$  at a precise applied voltage.

## 1. Introduction

There is a need for the development of small and cheap chemical gas sensor for detection of toxic and hazardous airborne pollutants. Sources of these molecules include, but are not limited to, paints, glues, exhaust pipes, solvents etc... Moreover, such technology is also suitable for the detection of trace amount of explosives.

One of the most promising and developed approach for this technology is based on the measurement of a resistance change between two electrodes as a chemical specie adsorbs on the medium in between them [1-4]. The sensing layer is usually a semiconducting metal oxide such as ZnO [1], CuO [2],  $TiO_2$  [3] and  $SnO_2$  [4]. The sensing layer is heated to a high temperature (about 300 °C) by a heater situated underneath which induces an increase in the concentration of reactive oxygen ions at the surface of the semiconductor [5]. Those anions react with the adsorbed pollutant

inducing a variation in electron conductivity in the material and thus a resistance variation.

Besides being completely compatible with conventional micro fabrication processes, this type of sensor also benefits from all of the various nanofabrication techniques developed for metal oxides to increase substantially their sensitivity [6]. However, to achieve any degree of selectivity, it is necessary to combine several of these sensors, in an array, with different sensing layers [7].

To achieve selectivity on a single sensor and at room temperature, this paper proposes to use the redox potential which is a characteristic of any chemical specie. To do that, the specie can be oxidized or reduced in an electrochemical cell configuration. When the applied voltage corresponds to the redox potential of the specie adsorbed on the electrodes, the electron exchange induced a change in current which can be measured. This signal allows for identification of the specie, as well as its quantification.

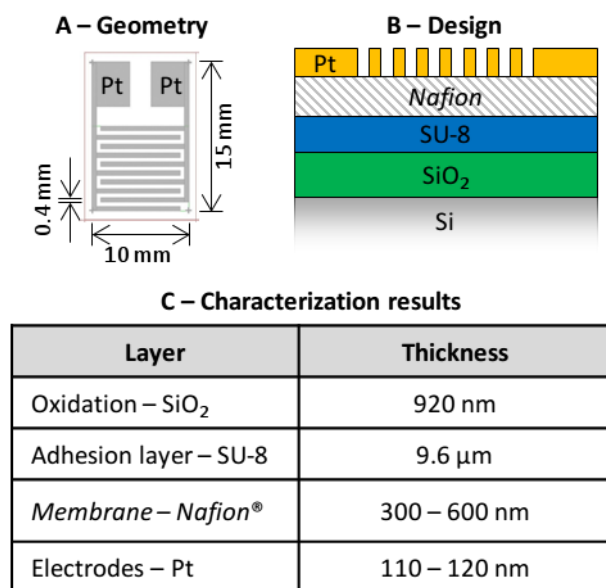


**Figure 1:** A – Electrodes geometry. B – Sensor cross-section (not to scale). C – Measured thicknesses of the different layers composing the sensor.

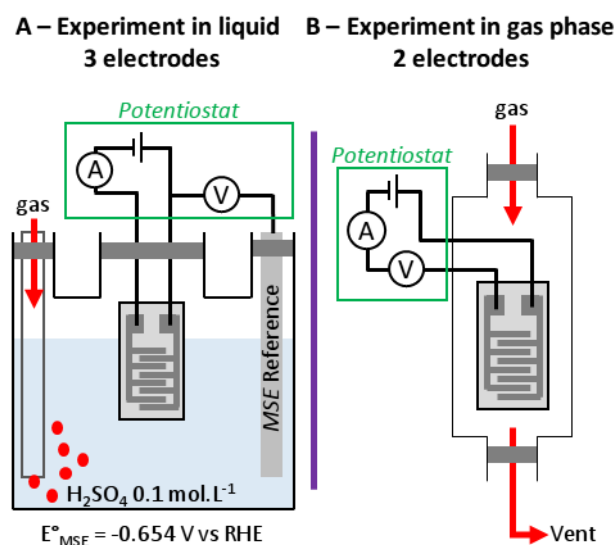


**Figure 2:** A – 3-electrode configuration for electrochemical characterization of the sensor in liquid. B – 2-electrodes configuration for the testing of the sensor in gas phase.

The main components of an electrochemical cell are the followings:

- One working and one counter electrode where the redox reaction will occur
- A reference electrode, to allow identification of the species involved in the redox reactions
- An electrolyte containing the species to be reduced or oxidized
- A membrane which role is to separate the two electrodes and conduct ions, resulting from the redox reactions, from one to the other.

The simplest design requires only two electrodes to achieve oxidation or reduction of chemical species. However, it is necessary to have a third electrode, the reference electrode, to be able to identify the specie being oxidized or reduced. This electrode is composed of a redox couple whose redox potential is well known and does not vary

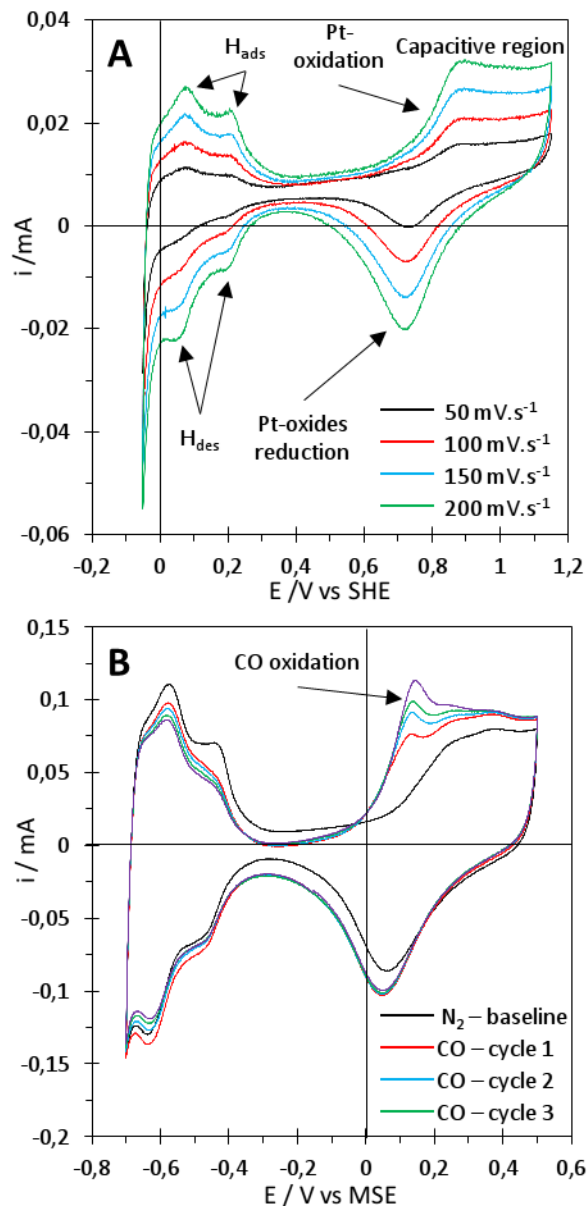


**Figure 3:** A – Cyclic voltammetry at different sweep rates in the 3-electrode configuration, in  $\text{H}_2\text{SO}_4$   $0.1 \text{ mol}\cdot\text{L}^{-1}$ . B – Cyclic voltammetry at  $200 \text{ mV}\cdot\text{s}^{-1}$  in  $\text{H}_2\text{SO}_4$  with different gases bubbling in the cell.

in the experimental conditions. It is by measuring the voltage between that reference electrode and the working electrode that it is possible to identify the species engaged in the electrochemical reaction on the working electrode thanks to the Nernst equation.

In order to detect molecules in the gas phase using this principle without using any liquid electrolyte, a fully solid state electrochemical cell must be developed. The main challenge is the incorporation of the membrane in the fabrication process.

Possible materials for the membrane include ionic conducting hydrogels [8], zirconia based materials [9] or ionic conductive polymers such as *Nafion*<sup>®</sup>. *Nafion* is a proton conducting membrane used in Proton Exchange Membrane Fuel Cells (PEMFC) which are reducing  $\text{O}_2$  and oxidizing  $\text{H}_2$  in acidic conditions [10]. One major advantage of *Nafion* is that, it conducts  $\text{H}^+$  at room temperature. It is a polymer whose monomer is composed of a *teflon*-like backbone chain and a sulfonic head. When hydrated, it forms clusters around water [11], and when acidified, the sulfonic groups allow proton transport [12].

Besides of being used in conventional fuel cells as described earlier, *Nafion* is also a promising material to be used in micro-fuel cells where it is used to separate the cathode and the anode while transporting protons [13]. The design developed in those devices, [14], has largely inspired the present work.

The sensor proposed in this paper demonstrates the feasibility of the electrochemical analysis of organic species dissolved in the gas phase. To obtain a fully solid state sensor, *Nafion* will be used as an ionic conductive electrolyte, and the electrodes will be made of Pt. Pt is chosen because of its well-studied electrochemical and electrocatalytic properties, and as its poisoning by CO in fuel cells is well documented [15,16].

## 2. Experimental Section

### Design of the sensor

The sensor has been designed with a few considerations in mind. First, the fabrication steps should impact the least possible the *Nafion* layer to keep its chemical integrity. In terms of redox reactions, the key features are the “triple points”, which are the interfaces where Pt, *Nafion* and the gas phase meet. With this in mind, the Pt electrodes do not need to be very thick, and it is anticipated that their thickness will not impact the sensitivity significantly. However, the main constraint for the geometry is the separation between the electrodes fingers because the ionic conductivity of *Nafion* drops drastically above  $500 \mu\text{m}$ .

Keeping the design simple is also necessary to prove that the proposed sensing mechanism might be compatible with mass production.

### Fabrication process

First, 100 mm diameter,  $525 \mu\text{m}$  thick Si wafers were processed with standard cleaning procedure in the following order: i) 90%  $\text{H}_2\text{SO}_4/\text{H}_2\text{O}_2$  (piranha), ii) 5:1:1  $\text{H}_2\text{O}:\text{H}_2\text{O}_2:\text{NH}_4\text{OH}$  iii) 50:1 HF iv) 5:1:1  $\text{H}_2\text{O}:\text{H}_2\text{O}_2:\text{HCl}$  (diffusion clean). A  $1 \mu\text{m}$  thick Si oxide layer is then grown on the substrate by wet oxidizing at  $1100 \text{ }^\circ\text{C}$  for 2 h 15 min.

Our studies have showed that *Nafion* adheres poorly to the  $\text{SiO}_2$  substrate, which is why a  $10 \mu\text{m}$  thick SU-8 2010 layer was first spin coated on the substrate at 1500 rpm for 5 sec and 3000 rpm for 15 sec. The layer is then exposed to a  $119 \text{ mJ}\cdot\text{cm}^{-2}$  dose of 365 nm UV light, baked at  $85 \text{ }^\circ\text{C}$  for 2 min to ensure hardening and drying of the SU-8 and developed. Prior to deposition of the *Nafion* layer, the SU-8 coated substrate is subjected to 30 sec of  $\text{O}_2$  plasma etching.

The *Nafion* layer is deposited by spin coating a D1021 *Nafion*<sup>®</sup> aqueous dispersion in three consecutive identical steps, which have been optimized to obtain a thickness of 300 nm, of 5 sec at 500 rpm followed by 30 sec at 1500 rpm. Each spin coating step is followed by

a 2 min back at 65 °C. The deposition process is finished by a 1h backing at 110 °C to ensure evaporation of all solvent. The electrodes are defined on the polymer coated wafer via a standard lift-off process. The HMDS treatment generally performed prior to the coating of the resist is skipped to avoid any chemical modification of the *Nafion* layer. A 3 μm thick SPR220-3 photoresist is spin coated and baked at 90 °C for 2 min. The wafer is then exposed to a 450 mJ·cm<sup>-2</sup> dose of 365 nm UV light, through a transparency mask displaying the geometry of the sensor showed on Figure 1A in a hard contact mode. The 100 nm thick Pt electrodes were deposited via e-beam evaporation and the resist was stripped in acetone.

Prior to characterization and testing, the *Nafion* layer needs to be rehydrated and acidified in order to have optimum proton conductivity. The sensor is thus immersed in a series of baths at 80 °C

for 15 min in each: i) H<sub>2</sub>O<sub>2</sub> 2%vol. in H<sub>2</sub>O, ii) H<sub>2</sub>SO<sub>4</sub> 0.1 mol·L<sup>-1</sup> iii) H<sub>2</sub>O. After that treatment the sensors are ready to be characterized and tested. A cross-section of the sensor is presented on Figure 1B.

#### Characterization and test methods

The topological characterization of the sensor was made with a profilometer and the results are presented in the table of Figure 1C. Concerning the *Nafion* layer, the measurement of its thickness revealed a quite important irregularity spanning from 300 to 600 nm across the wafer.

The sensors are first characterized as a conventional electrochemical cell in a three electrodes configuration. The test setup is presented in Figure 2A and represents the sensor with its two electrodes being respectively the working and counter electrode, connected to an external Mercury/Mercury Sulfate Electrode (MSE) reference electrode ( $E^{\circ}_{MSE} = -0.654$  V vs SHE) through a *Biologic*® SP-300 potentiostat. All three electrodes are immersed in a 0.1 mol·L<sup>-1</sup> H<sub>2</sub>SO<sub>4</sub> solution and cyclic voltammetry is performed between various potential limits and at different sweep rates. In cyclic voltammetry, the potential (in V) is applied and swept between the working and the counter electrodes. The corresponding current (in mA) flowing between the working and counter electrodes is recorded and plotted against the voltage measured between the working and the reference electrode.

Testing of the sensors for the detection of volatile pollutants are performed in a custom made test chamber presented on Figure 2B. The electrodes are connected to the same potentiostat in a two electrodes configuration. The test chamber is under constant gas flow from either N<sub>2</sub> or pure CO with a flow rate of 20 cm<sup>3</sup>·min<sup>-1</sup>. While the test chamber is under gas flow, the voltage is swept between the two electrodes of the sensor from -1.0 to 1.0 V with a 200 mV·s<sup>-1</sup> sweep rate.

#### Electrochemical characterization

The electrochemical characterization of the sensor consists of two experiments performed in the configuration of Figure 2A. The first one is done with N<sub>2</sub> bubbling in the cell, and the second one is with CO bubbling.

The experiment with N<sub>2</sub> is necessary to check that the Pt electrode surface is well exposed and available for redox reactions. The results are shown on Figure 3A where one can see a typical CV curve for polycrystalline Pt in acidic medium [17]. The quality of the Pt surface as well as the ionic conductivity of the *Nafion* are confirmed by the presence of all expected electrochemical signals. The observed signals are H adsorption/desorption located between 0 and 0.25 V vs SHE, the Pt oxide formation starting at 0.7 V vs SHE, the capacitive region plateau and the Pt oxides reduction peak at 0.7 V vs SHE. The experiment is conducted at several sweep rates from 50 mV·s<sup>-1</sup> to 200 mV·s<sup>-1</sup>. All electrochemical signals are increasing in current with the increasing sweep rate, which is expected for cyclic voltammetry.

The second electrochemical characterization is conducted in similar conditions but with CO bubbling. The resulting curve is showed on Figure 3B. One can see that the general shape of the curve is similar to the one obtained under N<sub>2</sub> but an oxidation peak appears at 0.15 V vs MSE. This peak corresponds to the oxidation of CO into CO<sub>2</sub> [16] according to its position on the potential scale when converted to the SHE scale ( $E(Pt) (CO_2/CO) \approx 0.8$  V vs SHE). The presence of this oxidation peak confirms that the sensor is indeed capable of detecting CO by measuring an increasing current at a specific applied potential corresponding to its redox potential. In addition to the presence of this oxidation peak, one can also see a slight decrease in the current at the H ads/des peaks. This phenomenon tends to confirm the nature of the oxidation of CO into CO<sub>2</sub> as the adsorption of CO on Pt occurs on the same catalytic sites as H [18].

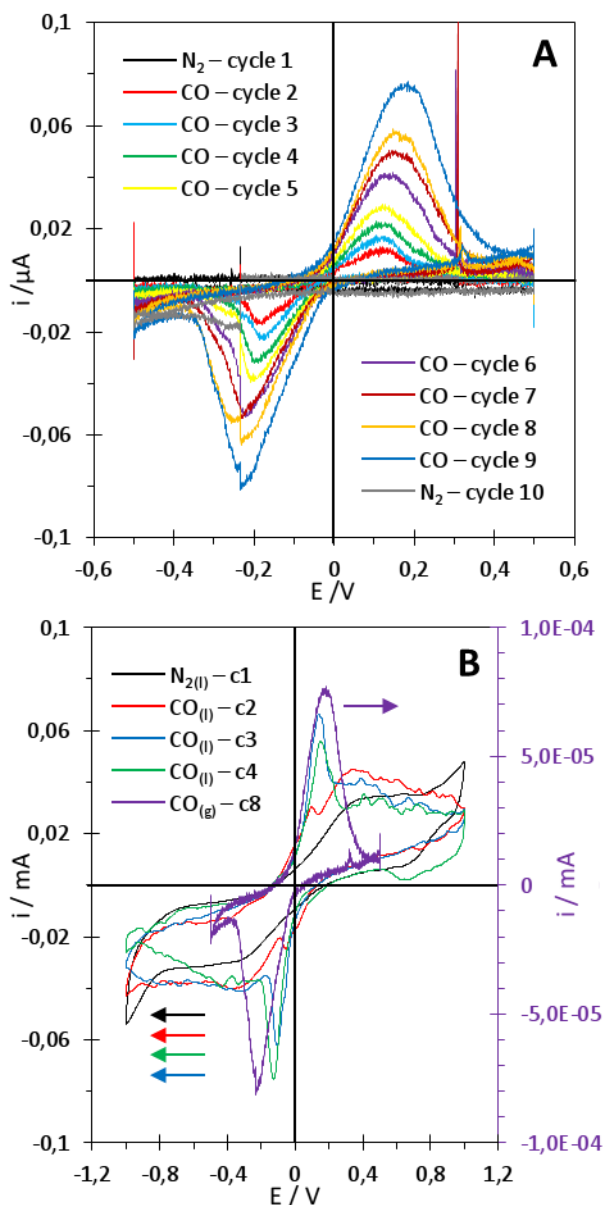


**Figure 4:** **A** – Cyclic voltammetry of the testing of the sensor in the 2-electrodes configuration in the gas phase under pure N<sub>2</sub> or CO flow. **B** – Superposition of cycle 9 of *A* and cyclic voltammetry obtained in liquid phase (H<sub>2</sub>SO<sub>4</sub> 0.1 mol·L<sup>-1</sup>), in a 2-electrodes configuration with pure CO bubbling.

### CO detection tests

As model pollutant CO was chosen, and its oxidation into CO<sub>2</sub> for validation of the electrochemical capabilities of the sensor. The experiment is conducted on the setup showed in Figure 2B. On Figure 4A, as the voltage is cycled between -0.5 and 0.5 V with a 200 mV·s<sup>-1</sup> sweep rate, the gas flow is alternatively switch from N<sub>2</sub> to CO and to N<sub>2</sub> again. In this configuration, the voltage is swept from one limit to the other in 5 s, which means that the observed changes in signal are happening on that time scale. The first cycles under N<sub>2</sub> allows to obtain a baseline to better identify the signal obtained under CO. The last cycles under N<sub>2</sub> are to confirm that the response time is around 5 s.

The initial curve obtained under N<sub>2</sub> flow, Figure 4A black line, shows low level of current as expected. When the CO flow is turned on, immediately an oxidation peak appears at 0.2 and -0.2 V with increasing current over cycles as the surface continues to be covered by CO. The charge of both peaks is almost identical, ≈0.3 μC, which shows that they are probably the signal of the same redox process happening alternatively on both electrodes as the polarization changes. As the gas flow is switch from CO to N<sub>2</sub> again, the oxidation signal disappears.

Although there is only CO flowing in the test cell, in the absence of a reference electrode, absolute identification cannot be done. In order to confirm that the observed signal is indeed CO oxidation into CO<sub>2</sub>, a similar experiment is performed in liquid environment..

The sensor is placed in the electrochemical cell with the same electrolyte, but this time without the reference electrode. Again, N<sub>2</sub> and CO are bubbled into the cell, and the resulting curves are shown in Figure 4B. In this two electrodes configuration, the shape of the curve observed previously is lost and becomes symmetrical with respect to 0 as is the curve obtained in the gas phase. The only shape which is observed under N<sub>2</sub> is the capacitive region of Pt. However, as CO is bubble in the cell, an oxidation peak appears at 0.2 and -0.2 V, just before the capacitive region, as it was observed on Figure 4B. These peaks can be attributed to CO oxidation, and its position in this configuration matches well with the position of the peaks observed in the gas phase experiment. Obtaining this curve confirms that the result from Figure 4A is indeed CO getting oxidized in CO<sub>2</sub> and thus that the sensor is capable of performing electrochemical measurements in gaseous conditions, and can identify the specie being adsorbed unlike conventional metal oxide based sensors measuring a change in resistance indicating that a specie is present, but cannot be identified [19].

### 4. Conclusion

In summary, the design and fabrication process of a micro electrochemical gas sensor were presented along with both topological and electrochemical characterizations. It has been showed that the sensor behaves as a typical working/counter electrodes couple when connected to an external reference electrode in a conventional electrochemical cell.

Testing of the sensor for the detection of CO as model pollutant has proved that the sensor is capable of electrochemical measurements in the gas phase.

To further improve the current sensor, the research effort is now focused on the implementation of a reference electrode in order to achieve identification of species directly in working conditions.

### 5. Acknowledgments

Authors would like to acknowledge the funding contribution of the French Department of Defense (DGA) and the BioX.

### 6. References

- [1] Q. Wan, Q. H. Li, Y. J. Chen, T. H. Wang, X. L. He, J. P. Li, and C. L. Lin, "Fabrication and ethanol sensing characteristics of ZnO nanowire gas sensors," *Appl. Phys. Lett.*, vol. 84, no. 18, pp. 3654–3656, May 2004.
- [2] S.-W. Choi, A. Katoch, J.-H. Kim, and S. S. Kim, "Remarkable Improvement of Gas-Sensing Abilities in p-type Oxide Nanowires by Local Modification of the Hole-Accumulation Layer," *ACS Appl. Mater. Interfaces*, vol. 7, no. 1, pp. 647–652, Jan. 2015.
- [3] T. Kida, M.-H. Seo, K. Suematsu, M. Yuasa, Y. Kanmura, and K. Shimano, "A Micro Gas Sensor Using TiO<sub>2</sub> Nanotubes to Detect Volatile Organic Compounds," *Appl. Phys. Express*, vol. 6, no. 4, p. 047201, Apr. 2013.
- [4] U. Hofer, H. Böttner, A. Felske, G. Kühner, K. Steiner, and G. Sulz, "Thin-film SnO<sub>2</sub> sensor arrays controlled by variation of contact potential—a suitable tool for chemometric gas mixture analysis in the TLV range," *Sens. Actuators B Chem.*, vol. 44, no. 1–3, pp. 429–433, Oct. 1997.
- [5] X. Liu, S. Cheng, H. Liu, S. Hu, D. Zhang, and H. Ning, "A Survey on Gas Sensing Technology," *Sensors*, vol. 12, no. 7, pp. 9635–9665, Jul. 2012.
- [6] H. Nguyen, C. T. Quy, N. D. Hoa, N. T. Lam, N. V. Duy, V. V. Quang, and N. V. Hieu, "Controllable growth of ZnO nanowires grown on discrete islands of Au catalyst for realization of planar-type micro gas sensors," *Sens. Actuators B Chem.*, vol. 193, pp. 888–894, Mar. 2014.
- [7] K. T. Ng, F. Boussaid, and A. Bermak, "A CMOS Single-Chip Gas Recognition Circuit for Metal Oxide Gas Sensor Arrays," *IEEE Trans. Circuits Syst. Regul. Pap.*, vol. 58, no. 7, pp. 1569–1580, Jul. 2011.
- [8] D. Kumar and S. A. Hashmi, "Ionic liquid based sodium ion conducting gel polymer electrolytes," *Solid State Ion.*, vol. 181, no. 8–10, pp. 416–423, Mar. 2010.
- [9] W. Sun, Z. Shi, M. Liu, L. Bi, and W. Liu, "An Easily Sintered, Chemically Stable, Barium Zirconate-Based Proton Conductor for High-Performance Proton-Conducting Solid Oxide Fuel Cells," *Adv. Funct. Mater.*, vol. 24, no. 36, pp. 5695–5702, Sep. 2014.
- [10] K. A. Mauritz and R. B. Moore, "State of Understanding of *Nafion*," *Chem. Rev.*, vol. 104, no. 10, pp. 4535–4586, Oct. 2004.
- [11] I. Pálkó, B. Török, G. K. S. Prakash, and G. A. Olah, "Dehydration–rehydration characteristics of *Nafion*-H, *Nafion*-H supported on silica and *Nafion*-H silica nanocomposite catalysts studied by Infrared Microscopy," *J. Mol. Struct.*, vol. 482–483, pp. 29–32, May 1999.
- [12] Y. Nagao, "Highly Oriented Sulfonic Acid Groups in a *Nafion* Thin Film on Si Substrate," *J. Phys. Chem. C*, vol. 117, no. 7, pp. 3294–3297, Feb. 2013.

- [13] A. D. Taylor, B. D. Lucas, L. J. Guo, and L. T. Thompson, "Nanoimprinted electrodes for micro-fuel cell applications," *J. Power Sources*, vol. 171, no. 1, pp. 218–223, Sep. 2007.
- [14] K. Shah, W. C. Shin, and R. S. Besser, "Novel microfabrication approaches for directly patterning PEM fuel cell membranes," *J. Power Sources*, vol. 123, no. 2, pp. 172–181, Sep. 2003.
- [15] Y. Wang, K. S. Chen, J. Mishler, S. C. Cho, and X. C. Adroher, "A review of polymer electrolyte membrane fuel cells: technology, applications, and needs on fundamental research," *Appl. Energy*, vol. 88, no. 4, pp. 981–1007, 2011.
- [16] T. Vidaković, M. Christov, and K. Sundmacher, "The use of CO stripping for in situ fuel cell catalyst characterization," *Electrochimica Acta*, vol. 52, no. 18, pp. 5606–5613, May 2007.
- [17] C. M. A. Brett and A. M. O. Brett, *Electrochemistry principles, methods, and applications*. Oxford; New York: Oxford University Press, 1993.
- [18] N. M. Marković, B. N. Grgur, C. A. Lucas, and P. N. Ross, "Electrooxidation of CO and H<sub>2</sub>/CO Mixtures on Pt(111) in Acid Solutions," *J. Phys. Chem. B*, vol. 103, no. 3, pp. 487–495, Jan. 1999.
- [19] Y.-F. Sun, S.-B. Liu, F.-L. Meng, J.-Y. Liu, Z. Jin, L.-T. Kong, and J.-H. Liu, "Metal Oxide Nanostructures and Their Gas Sensing Properties: A Review," *Sensors*, vol. 12, no. 3, pp. 2610–2631, Feb. 2012.